



Article

Utilization of Multi-Ionic Interaction of Yumoto Hot Springs for Enhancing the Moisturizing Properties of Hyaluronic Acid Sodium Salt

Keita Nakajima ¹, Tu Minh Tran Vo ² and Nur Adlin ^{1,*}

¹ Department of Science of Technology Innovation, Nagaoka University of Technology, 1603-1 Kamitomioka, Nagaoka, Niigata 940-2188, Japan; s203218@stn.nagaokaut.ac.jp

² Department of Energy and Environment Science, Nagaoka University of Technology, Niigata 940-2188, Japan; s217007@stn.nagaokaut.ac.jp

* Correspondence: nadlin@vos.nagaokaut.ac.jp

Abstract: Hot spring (HS) waters manifest diverse positive effects on the skin due to their unique chemical compositions. Sodium hyaluronate acid (HA) comprises N-acetylglucosamine and D-glucuronic acid, and distinguishes itself with superior qualities in skin regeneration, providing moisturizing and anti-aging benefits. The combination of HA with HS water is widely applied across ophthalmology, pneumology, nutrition, and cosmetics. This study delved into the application of HA in cosmetology, with a focus on its interaction with HS water and its effects on moisture retention and promoting wound healing. In particular, with the alkaline pH levels of the Yumoto HS, HA molecules may undergo dissociation to be ionized resulting in a negatively charged polymer and interacting with positively charged ions in the HS water through electrostatic interactions. The shifted peaks in the FTIR result and zeta potential shifts to a less negative region in the case of HA-HS compared to HA-DI indicate an ionic interaction between HS water and HA. Moisture tests confirmed the sustained hydration when HA is dissolved in HS water, underscoring its potential to improve skin hydration at certain concentrations, specifically at 0.5% and 1%. Additionally, MTT assay results demonstrated that HS water stimulates the growth of fibroblast cells compared to distilled water, implying its potential beneficial effect in wound healing. These findings suggested the multifaceted benefits of HAHS in skincare, highlighting its role in enhancing skin hydration and potentially accelerating wound healing processes, thus presenting avenues for the development of advanced cosmeceutical formulations.

Keywords: hot spring; sodium hyaluronate acid; moisturizing agent



Citation: Nakajima, K.; Tran Vo, T.M.; Adlin, N. Utilization of Multi-Ionic Interaction of Yumoto Hot Springs for Enhancing the Moisturizing Properties of Hyaluronic Acid Sodium Salt. *Polysaccharides* **2024**, *5*, 100–111. <https://doi.org/10.3390/polysaccharides5020008>

Academic Editor: Azizur Rahman

Received: 29 March 2024

Revised: 20 April 2024

Accepted: 30 April 2024

Published: 1 May 2024



Copyright: © 2024 by the authors. Licensee MDPI, Basel, Switzerland. This article is an open access article distributed under the terms and conditions of the Creative Commons Attribution (CC BY) license (<https://creativecommons.org/licenses/by/4.0/>).

1. Introduction

Hot springs (HSs) are a natural water source containing certain ions such as calcium, sodium, magnesium, potassium, chloride, and chemical substances [1]. The utilization of HS therapy, which operates without the need for chemicals and boasts minimal side effects [2], provides the benefit of conducting prolonged therapy safely without introducing potential health risks. Japan is rich in legends detailing the effects of HSs, and efforts have been made to scientifically substantiate these claims [3]. The Iwaki-Yumoto Hot Springs, boasting a history of over 1200 years, are considered one of Japan's three oldest HSs, alongside Arima and Dogo [4]. In some HS areas, the development and sale of cosmetics utilizing HS water have already been undertaken [5]. In this regard, the interaction between cosmetic ingredients and HS water components could be carefully considered. For example, utilizing balneotherapy with acidic HS water could be beneficial in managing skin symptoms during acute flare-ups of challenging cases of atopic dermatitis. Seventy patients engaged in a regimen of twice-daily 10 min baths in 42 degrees Celsius acidic HS water. Improvement in skin symptoms was observed in 76% of cases. Among

the 42 responders analyzed, balneotherapy resulted in the disappearance or reduction of staphylococcus aureus, detected on the skin surface, in 30 cases [6]. In the case of mild alkaline conditions, Comano HS water, with a pH of 7.5–7.6, decreases the expression of various cytokines and chemokines associated with psoriasis, suggesting potential efficacy in psoriasis treatment [7]. Kengo. I and Tohru. K demonstrated that HS water exhibited notable comfort and dermatological benefits when assessed for its effects on the skin and body conditions of capybaras [8]. Therefore, investigating the interaction between the quality of HS water and dermatological benefits is crucial for the cosmetics development industry. On the other hand, the idea of the aging exposome for the skin extends beyond a mere chronological progression, encompassing both external and internal influences [9]. In addition, HA serves as an important element in the extracellular matrix, experiencing a decline that initiates around the age of 25. The relevance of HA in dermatology has notably risen, due to its hygroscopic, rheological, and viscoelastic characteristics. HA has been utilized in the formulation of filler injections and incorporated into cosmeceuticals [10]. HA, known as a major polysaccharide found in cosmetics, is recognized for its safety and efficacy [11]. In previous studies, *in vivo* investigations were conducted using a dermocosmetic formulation (M89PF) comprising 80% Vichy mineral water, 5% *V. filiformis* lysate (cultivated in Vichy mineral water), 4% niacinamide (vitamin B3), 0.4% hyaluronic acid, and 0.2% vitamin E. The aim was to assess the clinical effectiveness in preventing and repairing stressed skin. Findings revealed that the M89PF dermocosmetic formulation significantly expedited skin renewal in comparison to untreated skin [12]. These substances have been found to have various effects on the skin, such as moisturizing and sterilizing effects. Furthermore, it has been reported that HA undergoes structural changes due to the ions present in aqueous solutions, such as its coagulating effect [13]. High molecular weight HA (HMW-HA) allows for tissue hydration, maintains osmotic balance, and stabilizes the extracellular matrix (ECM). It interacts with different receptor binding proteins, and its molecular weight can affect receptor affinity or cell uptake, resulting in varying outcomes. For instance, HMW-HA can suppress cell growth [14]. The positive charge of the ions is attracted to the negative charge of the carboxyl groups on HA. This electrostatic interaction can cause the HA chain to bend, twist, or fold [15]. When multivalent ions like Ca^{2+} or Mg^{2+} bind to HA chains or between different parts of the same chain, coiled structures are formed [16]. Interestingly, in the upper layer of the skin known as the stratum corneum, the quantity of hyaluronan rose when exposed to different metal chlorides, including NaCl, CaCl_2 , and MgCl_2 , with a concentration of 0.14 equivalents of metal ions during the penetration of 0.5% hyaluronan solutions into the skin [17]. Furthermore, the higher sodium content in HS water can enhance skin hydration by boosting the water retention capacity of HA. This ability to retain water keeps the extracellular matrix (ECM) hydrated, supporting the function of collagen and elastin fibers. Additionally, calcium ions can also facilitate cross-linking between HA molecules and collagen fibers, potentially stabilizing the ECM and enhancing its capacity to maintain skin structure [18,19]. To date, the detailed investigation regarding the interaction of cations and anions in HS water and HA molecules has not been explored yet. Therefore, this study aims to analyze the influence of ions in HS water on HA. This study is expected to uncover the potential of HS water in enhancing moisture retention on human skin. Furthermore, Fukushima Prefecture's Yumoto Onsen in Iwaki City contains multiple ions such as sodium ions, sulfate ions, chloride ions, and hydrogen carbonate ions, each exceeding 150 ppm. However, with a pH of 8.1, it has a relatively neutral water quality. Therefore, it was chosen for this experiment, as it is expected to have less impact on cosmetic ingredients compared to other HSs.

2. Materials and Methods

2.1. Materials

HS water was supplied by Joban Yumoto Onsen Co., Ltd. in Iwaki City, Fukushima Prefecture, Japan. The HS source was heated and collected from –800 m underground. HA

was purchased from Fujifilm Wako Pure Chemical Industries, Ltd., Osaka, Japan. All other reagents used in this study were of the analytical grade.

To determine the molecular weight of HA, HA powder was dissolved in a 2 mM phosphate-buffered saline (PBS) solution to obtain a 1 mg/mL HA solution. The molecular weight of the HA solutions was determined using gel permeation chromatography (GPC) with a refractive index detector (RID-10A; Shimadzu Corp., Tokyo, Japan). A mobile phase of 2 mM PBS at pH 7.2 was used, flowing at 0.5 mL/min through a GPC column (KD-806 M; Shodex; Showa Denko K.K.) maintained at 50 °C. The result showed that the M_w of HA was 5×10^6 Da.

2.2. Characterization of HS Water

Investigating the Properties of HS Water

Bacterial colony test: Plate count agar [20] was used to enumerate aerobic bacteria in deionized (DI) water and HS water. Sterile pipettes were utilized to apply 0.1 mL of each sample onto the surface of the agar petri dish with $\Phi = 85$ mm, spreading it evenly with a sterile glass spatula and incubating the plates at 37 ± 0.5 °C for 72 h. The bacterial count was computed per milliliter of the sample by multiplying the average colony count per plate by the reciprocal of the dilution factor applied. The results were presented as colony-forming units per milliliter (CFU/mL).

Biocompatibility tests: Mouse NIH/3T3 fibroblast cells were cultivated in an environment maintained at 37 °C, 95% relative humidity, and 5% CO₂ atmosphere. Dulbecco's modified Eagle's medium (DMEM) supplemented with 10% fetal bovine serum (FBS) and 1% penicillin/streptomycin constituted the culture medium. The cell count was determined using a hemocytometer and then diluted to a concentration of 4×10^4 cells/mL. Next, the cell solution was prepared in Falcon Easy Grip™ tissue culture dishes measuring 35 mm by 10 mm, with a cell density of 8×10^3 cells/cm². The cell proliferation and morphology of PBS (control sample), HS water, and DI water samples were evaluated after incubation for 6, 24, and 48 h, employing a phase-contrast inverted light microscope (ECLIPSE TS100-F, Nikon, Japan). Cell density was determined by counting randomly 5 images of each condition and performing the average cell density calculations.

The assessment of in vitro cytotoxicity for HS water and DI water was conducted through the MTT (3-(4,5-dimethylthiazol-2-yl) 2,5-diphenyl tetrazolium bromide) assay [21,22]. A cell concentration of 4000 cells/well was seeded into 96-well plates and incubated for 24 h before introducing samples into each well. After 24 h, 200 μ L of HS water and DI water were added to each 96-well plate. The cells were then further incubated for 6 h, 24 h, and 48 h. Subsequently, MTT (5 mg/mL) was introduced to each well and incubated for 4 h under the same conditions as the earlier cell culture procedure. Cell viability was determined by measuring absorbance at a wavelength of 550 nm using a microplate reader (Elx808, Biotek, Washington, DC, USA), and the results were compared with control cells that were seeded with PBS.

The experiments were conducted a minimum of three times and statistically analyzed using the Origin 2018 software. The results were presented as average values with accompanying standard deviations to indicate data variability.

2.3. Characterization of HS Water Combined with HA

The viscosity tests of HS-HA and DI-HA mixtures at different concentrations of HA ranging from 0.5% to 3% were performed using a rheometer (Physica MCR 301, Anton Paar, Graz, Austria). A conc-plate geometry (diameter 25 mm) was utilized in all rheological tests. To confirm the ionic interaction between HS water and HA, the determination of the zeta potential was carried out using a Photal Otsuka electronics setup with an ELSZ1 NGK flow cell.

The chemical structures of HA in DI water and HS water were examined using Fourier-transform infrared (FTIR) spectroscopy with a JASCO FT/IR-4100 instrument

(JASCO Corporation, Tokyo, Japan). Spectra were recorded in the range of 4000–1000 cm^{-1} and an average of 32 scans were collected.

The evaluation of moisture retention properties in the comparison of HS-HA and DI-HA was conducted using a moisture checker (Scalar, Tokyo, Japan) within a controlled environment (22 ± 1 °C, $37 \pm 1.0\%$ RH). A series of 0.5% to 3% *w/v* HA solutions was prepared in HS water and DI water; the control samples were without HA. A total of 20 μL of each solution was applied to the skin surface, allowing the solution to dry under the air. The moisture content on 24-year-old male skin was measured by capturing three data points per sample area at intervals of 1, 10, 20, 30, and 60 min.

3. Results and Discussion

3.1. The Quality of Yumoto Onsen HS Water

The bacterial count per milliliter of the sample was determined by multiplying the average number of colonies per plate by the reciprocal of the dilution factor employed. The result was expressed as colony-forming units per milliliter (CFU/mL). This method holds significant relevance in cosmetic microbiology, where ensuring the product safety is paramount. The results indicated the presence of 2.9×10^5 CFU/mL in the control sample (Figure 1). However, no visible colonies were observed on the agar gel surface treated with autoclaved water (sterilized water) and HS water. This suggests that HS water effectively inhibited bacterial growth, highlighting its potential as a natural bactericidal agent in cosmetic formulations.

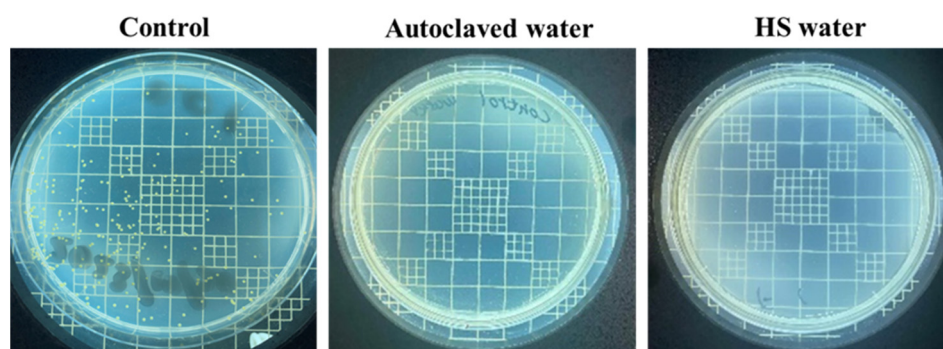


Figure 1. Appearance of the bacterial colonies observed on agar plates after 72 h incubation. A total of 0.1 mL of the control sample containing 100 CFU/mL (diluted by a factor of 100), along with autoclaved water and HS water, were inoculated onto agar plates.

Figure 2 depicts images of the morphology and density of NIH/3T3 fibroblast cells at various time intervals. The findings indicated an increase in the number of surviving cells with prolonged cultivation time across all cases. At the 6 h mark of cell culture, the images captured from HS water exhibited a higher cell density with 1.72×10^4 cells/ cm^2 compared to the control sample using PBS and DI water under the same conditions. This trend became more pronounced after 48 h cultivation periods, where the cell density of DI water and HS water reached 3.86×10^5 cells/ cm^2 . This result showed that HS water might stimulate cell proliferation more efficiently than in the control conditions (using PBS and DI water) due to its distinctive composition, which often includes various minerals and ions (Table 1). These multi-ionic constituents have the potential to interact with cellular processes and signaling pathways, potentially affecting cell behavior and proliferation. Specific ions found in HS water, such as calcium, magnesium, and potassium, have been demonstrated to modulate ion channels and transporters within cell membranes [23]. Additionally, the presence of multi-ionic compounds in HS water could create a microenvironment closer to physiological conditions compared to pure water [24]. Moreover, in the control sample, fibroblasts exhibited a spindle-shaped morphology as individual cells. In contrast, exposure to DI water and especially HS water prompted a noticeable shift towards a round-shaped appearance. This alteration in morphology indicates changes in cell behavior and could

reflect differences in cell signaling pathways or responses to environmental cues offered by the various types of water [25].

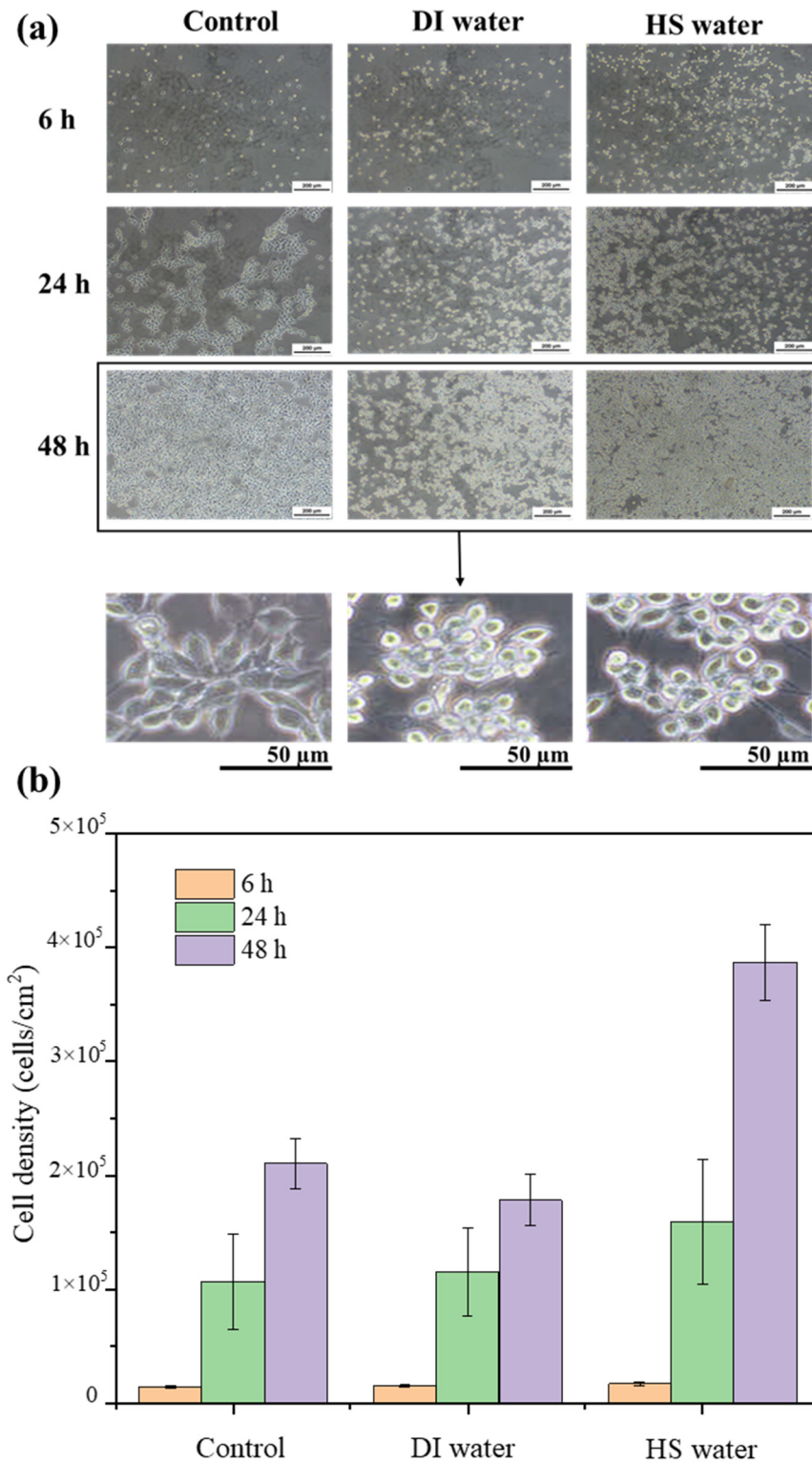


Figure 2. The distribution of fibroblast cells was observed and captured using phase-contrast light microscopy (a). Cell density plots (b) from the control sample with PBS as the sample, DI water, and HS water.

Table 1. The ionic components of HS water \diamond .

Cations	Conc. (mg/kg)	mval % *	Anions	Conc. (mg/kg)	mval % *
Li ⁺	0.3	0.15	F ⁻	4.8	0.91
Na ⁺	544.4	84.72	Cl ⁻	648.8	65.99
K ⁺	7.1	0.65	Br ⁻	2.3	0.10
NH ₄ ⁺	0.7	0.14	I ⁻	0.4	0.01
Mg ²⁺	2.5	0.74	HS ⁻	7.2	0.79
Ca ²⁺	75.8	13.54	S ₂ O ₃ ²⁻	4.7	0.30
Si ²⁺	0.7	0.06	SO ₄ ²⁻	309.6	23.24
-	-	-	HCO ₃ ⁻	146.5	8.66

\diamond The data is referenced from Joban Yumoto Onsen Co., Ltd., Japan. * Millival (mval) is a unit that expresses the concentration of ionic species dissolved in 1 kg of HS water and is a unit of 1/1000 of the unit of 1 val (val). Millival % is the ratio of the millival value of a certain cation or anion to the millival value of all cations or anions.

After 6 h of incubation, there was a slight increase in the number of viable cells, ranging from 8500 to 9400 and 11,000 cells/well for the control, DI water, and HS water conditions, respectively. However, cells treated with DI water exhibited lower growth, around 13,000 cells/well compared to 16,000 cells/well for the control after 24 h, as shown in Figure 3. Over the subsequent 48 h of incubation, NIH/3T3 cell survival experienced a significant increase, particularly evident with HS water, of over 30,000 cells/well for cell proliferation. As mentioned above, it was because the multi-ions in HS water bear a closer resemblance to the electrolyte balance encountered in biological fluids. This similarity may provide cells with the necessary nutrients and signaling cues to support optimal growth [26].

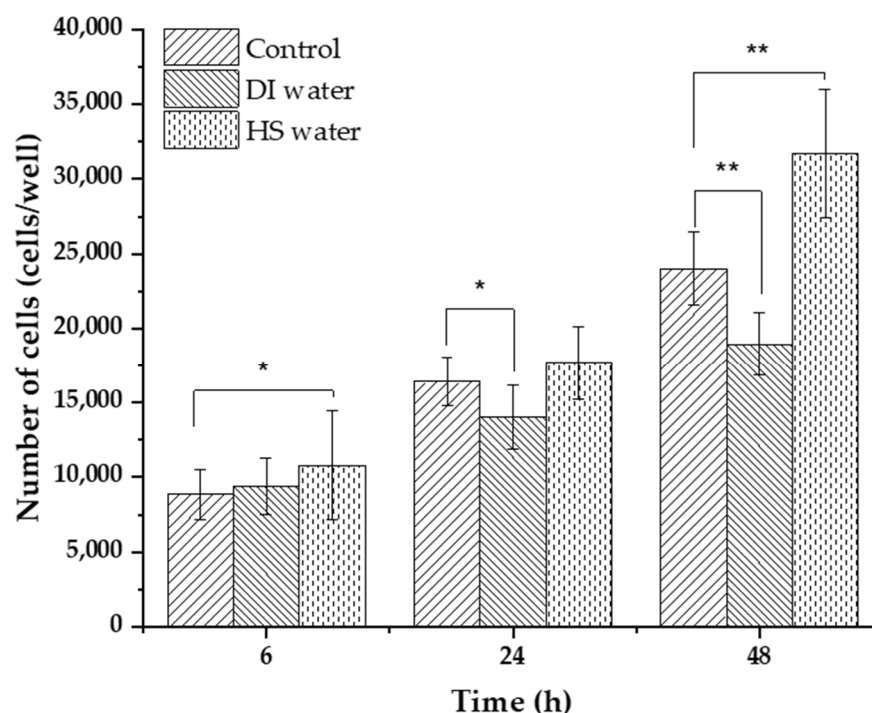


Figure 3. The cell counts per well plate of the control sample, DI water, and HS water after 6 h, 24 h, and 48 h of incubation were subjected to statistical analysis. Significance was determined with *p*-values denoted as follows: * *p* < 0.05 and ** incubation were subjected to statistical analysis. Significance was *p* < 0.001.

3.2. Incorporation of HS Water in Combination with HA as a Moisturizing Agent

The changing of apparent viscosity with the shear rate is depicted in Figure 4a. The apparent viscosity of all samples reduced as the shear rate (0.1–1000 s⁻¹) increased; the samples behaved as non-Newtonian pseudoplastic fluids [27]. This shear-thinning effect was

attributable to the HA intermolecular forces being weaker as the shear rate increased [28]. The viscosity of the HA solution dissolved in DI water was higher compared to HA dissolved in HS water at equivalent concentrations. This difference became more evident as the HA concentration increased up to 3%. Specifically, at a shear rate of 0.1 s^{-1} , the viscosity of HA dissolved in HS water increased from 1 Pa.s to over 300 Pa.s as the HA concentration rose from 0.5% to 3%. HA is a polyelectrolyte which is composed of repeating polymeric disaccharides of D-glucuronic acid and N-acetyl-D-glucosamine linked by a glucuronidic β (1 \rightarrow 3) bond, as depicted in Scheme 1. The rheological characteristics in HA aqueous solutions are also affected by factors such as ionic strength, pH, and temperature [29]. The presence of ions like Na^+ (84.72 mval%) and Cl^- (65.99 mval%) in the solution leads to ion hydration, where water molecules form hydration shells around the ions. This hydration reduces the effective interaction between sodium hyaluronate molecules, resulting in lower viscosity compared to water without these main ions.

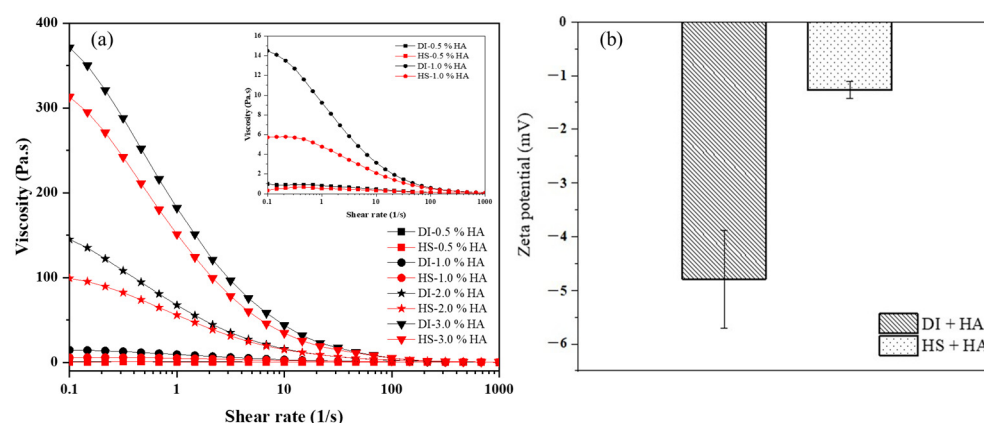
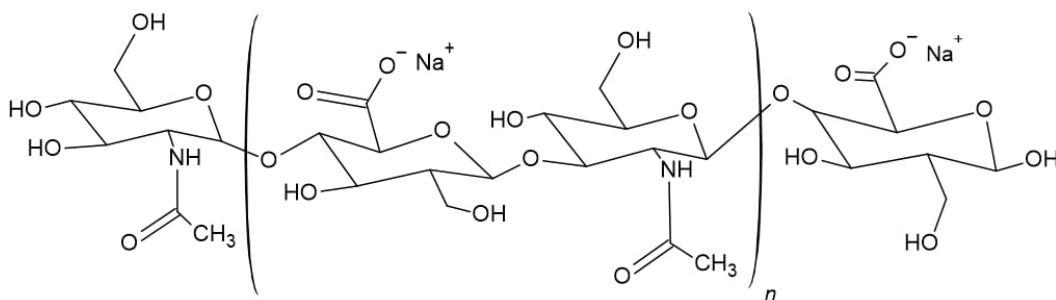


Figure 4. The viscosity of HA solutions prepared in DI water and HS water at different concentrations ranging from 0.5% to 3% (a) and zeta potential values of HA in DI water and HS water (b).



Scheme 1. Chemical structure of HA.

As depicted in Figure 4b, the zeta potential value of HA dissolved in HS water was less negative compared to HA dissolved in DI water, with values of -1.2 mV and -4.8 mV , respectively, indicating a salt shielding effect [30]. This is evidence that electrostatic forces were formed with the addition of Na^+ , Ca^{2+} , Cl^- , SO_4^{2-} , and HCO_3^- ions. In addition, HS water typically contains a higher concentration of ions and minerals compared to regular water. These ions can interact with the charged groups present in HA molecules. These interactions can lead to the formation of complexes between HA and the ions, stabilizing the colloidal structure of HA in HS water [31], as displayed in Figure 5b, which aligns with earlier discoveries (outlined in Table 2). In contrast, the lower ion concentration in DI water results in HA existing in a hydrated form instead, with the inter- and intra- H bonding (Figure 5a). Furthermore, the viscosity of HA substantially decreases, also indicating a reduction in the interactions among the polymer chains when HA was dissolved in HS water. As a result, negative values of zeta potential were close to zero charge. This observation indicates a decrease in the degree of dissociation of the hyaluronic acid molecule.

It is hypothesized that ions in the solution reduce the dissociation of molecules that were initially repelled electrostatically, thereby diminishing the interaction between polymer chains. Consequently, this leads to a decrease in viscosity and an increase in zeta potential.

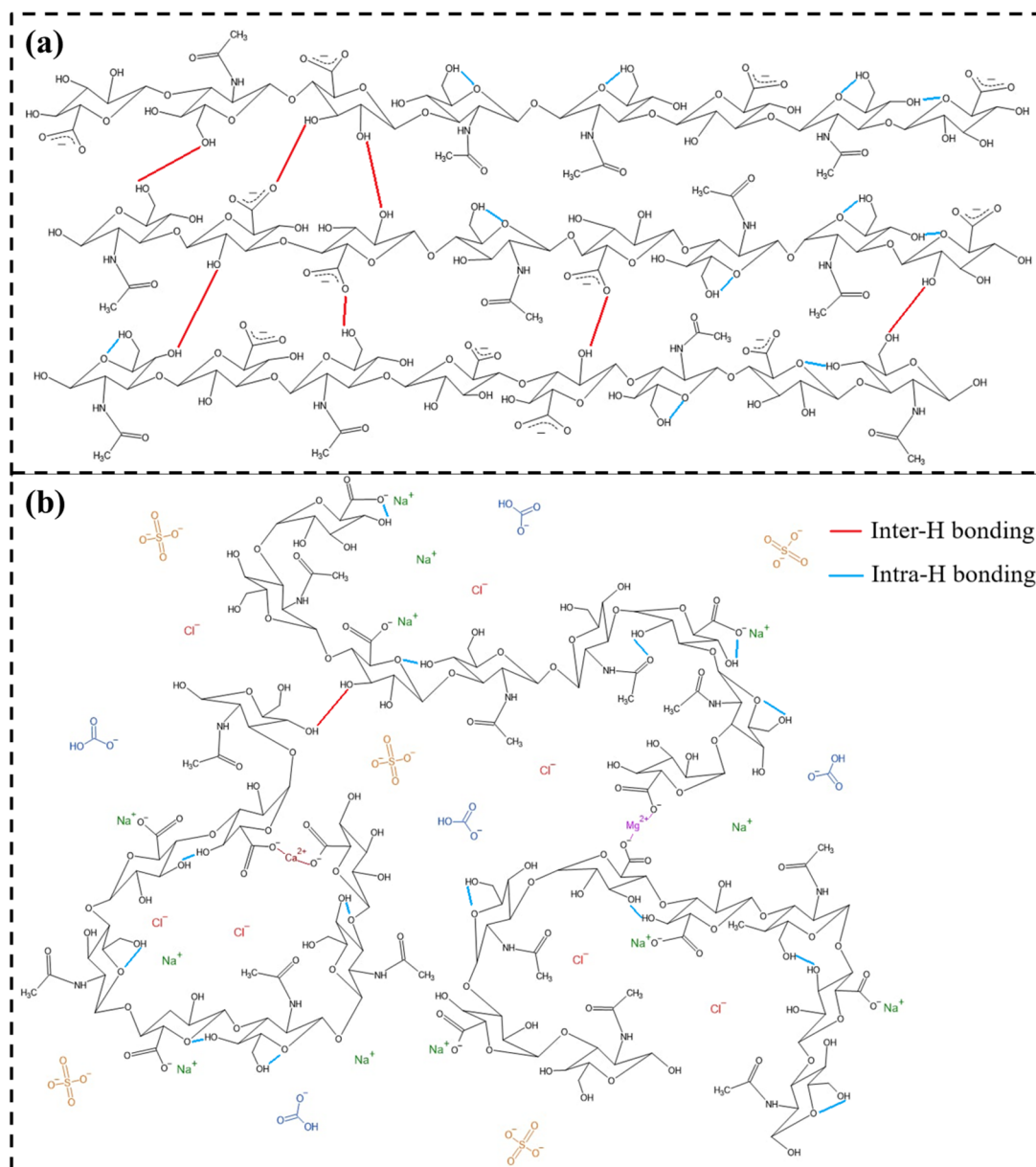


Figure 5. The proposed interaction of HA molecules dissolved in (a) DI and (b) HS water.

Figure 6 depicts the FTIR spectra of HA, where broad absorption bands were observed around 3414 , 3389 , and 3394 cm^{-1} corresponding to the stretching of the OH/NH groups of HA powder, HA in DI water, and HA in HS water, respectively. The peak shifted to a lower position when HA was dissolved in DI water, suggesting the formation of inter- and intra-hydrogen bonds between HA and water molecules. However, this phenomenon was less noticeable in HS water, as the presence of both cations and anions could interact with HA, potentially limiting the formation of hydrogen bonds between HA and water. Additionally, the C-H bonds of CH₂ were shown at 2945 cm^{-1} . Spectral features indicative of carboxylate anions were present in HA, with absorption bands at 1616 and 1409 cm^{-1} , attributed to the asymmetric and symmetric stretching vibrations of carboxylate anions (related to the C=O bond and C-O bond of the -COONa group). Moreover, characteristic peaks at 1592 and 1038 cm^{-1} were observed, corresponding to the vibrations of amide

II (mainly from N-H bending and C-N stretching vibrations) [32] and the C–O–C bond, respectively, indicating the presence of amide bonds in HA [33]. Compared to HA powder, when HA is dissolved in DI water, it exhibits a lower position at 1611 cm^{-1} for the COO^- group, indicating a strong interaction with water molecules. Conversely, in HS water, HA displayed a shift to higher wavenumbers. This shift was attributed to the abundant multi-ions, particularly sodium ions, present in HS water, which caused a reduction in the COO^- groups, leading to their existence in the COONa form.

Table 2. Comparison of the ionic interaction of different M_w of HA and their applications.

Ions	M_w of HA *	Key Outcomes	Reference
Mg^{2+} and Cl^-	High M_w	Non-invasive delivery of hyaluronan into the stratum corneum.	[17]
Na^+ , NH_4^+ , Mg^{2+} , Li^+ , SO_4^{2-} , Cl^- , SCN^-	High and low M_w	Diffusion coefficients for solutions with sodium hyaluronate and salts inform modeling for pharmaceutical and engineering diffusion.	[34]
Ca^{2+} and Cl^-	N.A	The binding of the calcium ions weakens the intramolecular hydrogen-bond network of hyaluronan, increasing the flexibility of the polymer chain.	[35]
Na^+ and Cl^-	Low M_w	Hyaluronic acid-coated aggregated vesicle formation.	[36]
HS water (Na^+ , Ca^{2+} , Mg^{2+} , SO_4^{2-} , Cl^-)	High M_w	Reduction in viscosity of HA solution in the presence of multi-ions in HS water; utility as an essential moisturizer.	This study

* High molecular weight: $M_w > 1\text{ MDa}$. Low molecular weight: $M_w < 1\text{ MDa}$.

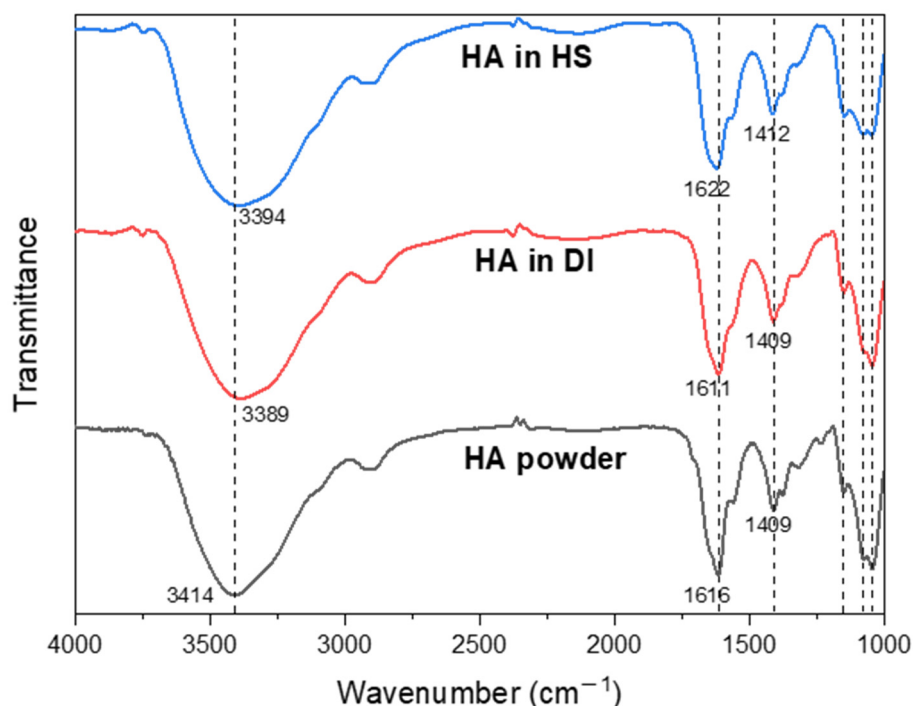


Figure 6. FTIR spectra of HA powder, HA in DI water, and HA in HS water.

Figure 7a displays images demonstrating the application of HA solutions ranging from 0% to 3% concentration in both DI water and HS water onto the skin. In Figure 7b,c,

the temporal changes in skin surface moisture percentage at the regions coated with HA solutions are presented. Initially, the moisture retention of the skin surface measured approximately 28% for the control sample without HA. However, upon application of a 0.5% aqueous HA solution, the moisture retention values increased to nearly 33% and 36% during the initial 10 min, decreasing to approximately 29% and 31.5% after 60 min for DI water and HS water, respectively. Notably, the HA-HS conditions exhibited higher moisture retention percentages compared to HA-DI across all HA concentration ranges from 0.5% to 3%. The hygroscopic properties of HA [37] enable it to attract and retain water molecules from the surrounding environment effectively, thus hydrating the skin by drawing moisture from the air and deeper layers of the skin. Additionally, HA plays a role in supporting the skin's natural barrier function by maintaining adequate moisture levels in the outermost layer of the skin [38]. The combination of HA and HS water may enhance the hydration properties of both substances, creating synergistic effects on the skin to optimize hydration levels. In the case of HA-HS, moisture values were enhanced with increasing HA content up to 1% but decreased at higher HA concentrations of 2% and 3% due to the higher viscosity of the HS water solution. This higher viscosity resulted in less absorption into the skin and the formation of a thin dry layer on the skin surface, which could impede the skin's ability to breathe, disrupt its natural functions, and ultimately result in dryness. Furthermore, exceeding a certain amount of HA, by over 1%, may lead to the loss of skin moisture because HA could draw moisture from deeper layers of the skin, exacerbating dryness rather than hydrating the skin.

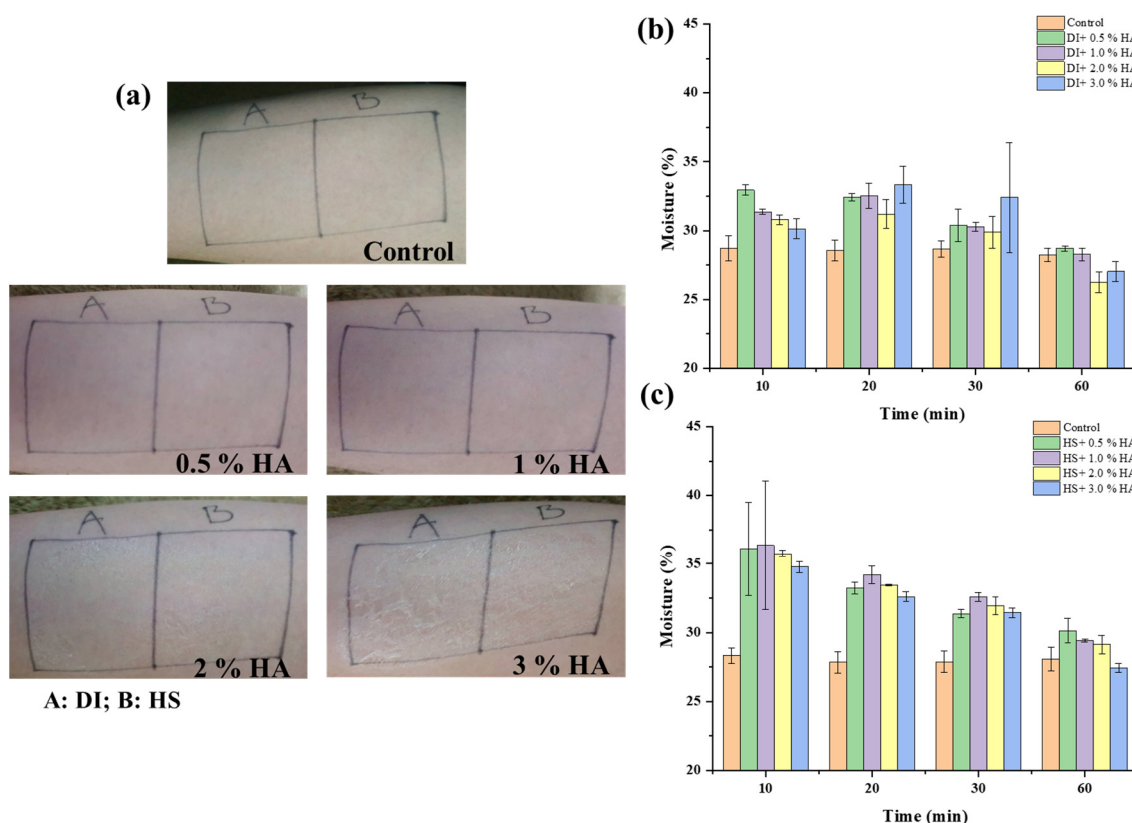


Figure 7. The assessment of skin appearance (a). In vivo moisture retention percentage tests of the skin surface were conducted by applying HA solutions dissolved in DI water (b) and HS water (c) over a period ranging from 10 min to 60 min.

4. Conclusions

This study reports on the promising combination of HA and HS water in cosmetology and its impact on moisture retention and the potential promotion of wound healing. The shift towards a less negative region in zeta potential for HA-HS compared to HA with

DI water indicated an ionic interaction between HS water and HA. It was noted that a significant enhancement in moisture retention was observed, reaching 36% during the initial 10 min of the HA-HS solution, indicating its potential to enhance skin moisture levels, particularly at concentrations of 0.5% and 1%. Moreover, MTT assays illustrated that HS water encourages the proliferation of fibroblast cells in comparison to DI water. After 48 h of incubation, NIH/3T3 cell survival experienced a significant increase, particularly evident with HS water, of over 30,000 cells/well. These findings underscored the various benefits of HA-HS in skincare, emphasizing its ability to improve skin hydration and potentially expedite wound healing processes, thereby paving the way for the development of more advanced cosmeceutical formulations.

Author Contributions: K.N.: conceptualization, methodology, writing—original draft preparation; T.M.T.V.: formal analysis, writing—original draft preparation; N.A.: validation, writing—review and editing. All authors have read and agreed to the published version of the manuscript.

Funding: This research received no external funding.

Institutional Review Board Statement: Not applicable.

Data Availability Statement: Data are contained within the article.

Acknowledgments: This research was supported by Joban Yumoto Onsen Co., Ltd.

Conflicts of Interest: The authors declare no conflicts of interest.

References

1. Des Marais, D.J.; Walter, M.R. Terrestrial Hot Spring Systems: Introduction. *Astrobiology* **2019**, *19*, 1419–1432. [[CrossRef](#)] [[PubMed](#)]
2. Matz, H.; Orion, E.; Wolf, R. Balneotherapy in Dermatology. *Dermatol. Ther.* **2003**, *16*, 132–140. [[CrossRef](#)] [[PubMed](#)]
3. Wang, H. A review of research papers on the health-promoting effects of hot springs reported in Japanese over the past 20 years. *Jpn. Hot Spring Phys. Soc.* **2006**, *69*, 81–102. [[CrossRef](#)]
4. Koito Ryokan. Available online: <https://koito-inn.co.jp/en/> (accessed on 10 April 2024).
5. Biondi, N.; Martina, M.R.; Centini, M.; Anselmi, C.; Tredici, M.R. Hot Springs Cyanobacteria Endowed with Biological Activities for Cosmetic Applications: Evaluation of On-Site Collected Communities and Isolated Strains. *Cosmetics* **2023**, *10*, 81. [[CrossRef](#)]
6. Kubota, K.; Machida, I.; Tamura, K.; Take, H.; Kurabayashi, H.; Akiba, T.; Tamura, J. Treatment of Refractory Cases of Atopic Dermatitis with Acidic Hot-Spring Bathing. *Acta Derm. Venereol.* **1997**, *77*, 452–454. [[CrossRef](#)] [[PubMed](#)]
7. Chiarini, A.; Dal Pra, I.; Pacchiana, R.; Zumiani, G.; Zanoni, M.; Armato, U. Comano's (Trentino) Thermal Water Interferes with Interleukin-6 Production and Secretion and with Cytokeratin-16 Expression by Cultured Human Psoriatic Keratinocytes: Further Potential Mechanisms of Its Anti-Psoriatic Action. *Int. J. Mol. Med.* **2006**, *18*, 1073–1079. [[CrossRef](#)] [[PubMed](#)]
8. Inaka, K.; Kimura, T. Comfortable and Dermatological Effects of Hot Spring Bathing Provide Demonstrative Insight into Improvement in the Rough Skin of Capybaras. *Sci. Rep.* **2021**, *11*, 23675. [[CrossRef](#)]
9. Krutmann, J.; Bouloc, A.; Sore, G.; Bernard, B.A.; Passeron, T. The Skin Aging Exposome. *J. Dermatol. Sci.* **2017**, *85*, 152–161. [[CrossRef](#)] [[PubMed](#)]
10. Vasvani, S.; Kulkarni, P.; Rawtani, D. Hyaluronic Acid: A Review on Its Biology, Aspects of Drug Delivery, Route of Administrations and a Special Emphasis on Its Approved Marketed Products and Recent Clinical Studies. *Int. J. Biol. Macromol.* **2020**, *151*, 1012–1029. [[CrossRef](#)]
11. Becker, L.C.; Bergfeld, W.F.; Belsito, D.V.; Klaassen, C.D.; Marks, J.G.; Shank, R.C.; Slaga, T.J.; Snyder, P.W.; Cosmetic Ingredient Review Expert Panel; Andersen, F.A. Final Report of the Safety Assessment of Hyaluronic Acid, Potassium Hyaluronate, and Sodium Hyaluronate. *Int. J. Toxicol.* **2009**, *28*, 5–67. [[CrossRef](#)]
12. Mourelle, M.L.; Gómez, C.P.; Legido, J.L. Hydrobiome of Thermal Waters: Potential Use in Dermocosmetics. *Cosmetics* **2023**, *10*, 94. [[CrossRef](#)]
13. Al-Khateeb, R.; Prpic, J. Hyaluronic Acid: The Reason for Its Variety of Physiological and Biochemical Functional Properties. *Appl. Clin. Res. Clin. Trials Regul. Aff.* **2019**, *6*, 112–159. [[CrossRef](#)]
14. Girish, K.S.; Kemparaju, K. The Magic Glue Hyaluronan and Its Eraser Hyaluronidase: A Biological Overview. *Life Sci.* **2007**, *80*, 1921–1943. [[CrossRef](#)] [[PubMed](#)]
15. Taweechat, P.; Pandey, R.B.; Sompornpisut, P. Conformation, Flexibility and Hydration of Hyaluronic Acid by Molecular Dynamics Simulations. *Carbohydr. Res.* **2020**, *493*, 108026. [[CrossRef](#)] [[PubMed](#)]
16. Svarca, A.; Grava, A.; Dubnika, A.; Ramata-Stunda, A.; Narnicks, R.; Aunina, K.; Rieksta, E.; Boroduskis, M.; Jurgelane, I.; Locs, J.; et al. Calcium Phosphate/Hyaluronic Acid Composite Hydrogels for Local Antiosteoporotic Drug Delivery. *Front. Bioeng. Biotechnol.* **2022**, *10*, 917765. [[CrossRef](#)] [[PubMed](#)]

17. Fujii, M.Y.; Okishima, A.; Ichiwata, H.S.; Oka, T. Biocompatible Topical Delivery System of High-Molecular-Weight Hyaluronan into Human Stratum Corneum Using Magnesium Chloride. *Sci. Rep.* **2023**, *13*, 10782. [[CrossRef](#)] [[PubMed](#)]
18. Jiang, Y.-H.; Lou, Y.-Y.; Li, T.-H.; Liu, B.-Z.; Chen, K.; Zhang, D.; Li, T. Cross-Linking Methods of Type I Collagen-Based Scaffolds for Cartilage Tissue Engineering. *Am. J. Transl. Res.* **2022**, *14*, 1146–1159. [[PubMed](#)]
19. Fan, Y.; Choi, T.-H.; Chung, J.-H.; Jeon, Y.-K.; Kim, S. Hyaluronic Acid-Cross-Linked Filler Stimulates Collagen Type 1 and Elastic Fiber Synthesis in Skin through the TGF- β /Smad Signaling Pathway in a Nude Mouse Model. *J. Plast. Reconstr. Aesthetic Surg.* **2019**, *72*, 1355–1362. [[CrossRef](#)] [[PubMed](#)]
20. Buchbinder, L.; Baris, Y.; Alff, E.; Reynolds, E.; Dillon, E.; Pessin, V.; Pincus, L.; Strauss, A. Studies to Formulate New Media for the Standard Plate Count of Dairy Products. *Public Health Rep. (Wash. D. C. 1896)* **1951**, *66*, 327–340. [[CrossRef](#)]
21. Panda, P.K.; Sadeghi, K.; Park, K.; Seo, J. Regeneration Approach to Enhance the Antimicrobial and Antioxidant Activities of Chitosan for Biomedical Applications. *Polymers* **2023**, *15*, 132. [[CrossRef](#)]
22. Tran Vo, T.M.; Nakajima, K.; Potiyaraj, P.; Kobayashi, T. In Situ Sono-Rheometric Assessment of Procaine-Loaded Calcium Pectinate Hydrogel for Enhanced Drug Releasing under Ultrasound Stimulation. *Int. J. Biol. Macromol.* **2024**, *262*, 130164. [[CrossRef](#)]
23. Liu, H.-W.; Hou, P.-P.; Guo, X.-Y.; Zhao, Z.-W.; Hu, B.; Li, X.; Wang, L.-Y.; Ding, J.-P.; Wang, S. Structural Basis for Calcium and Magnesium Regulation of a Large Conductance Calcium-Activated Potassium Channel with B1 Subunits*. *J. Biol. Chem.* **2014**, *289*, 16914–16923. [[CrossRef](#)] [[PubMed](#)]
24. Mu, Y.; Du, Z.; Xiao, L.; Gao, W.; Crawford, R.; Xiao, Y. The Localized Ionic Microenvironment in Bone Modelling/Remodelling: A Potential Guide for the Design of Biomaterials for Bone Tissue Engineering. *J. Funct. Biomater.* **2023**, *14*, 56. [[CrossRef](#)] [[PubMed](#)]
25. Ballester-Beltrán, J.; Biggs, M.J.P.; Dalby, M.J.; Salmerón-Sánchez, M.; Leal-Egaña, A. Sensing the Difference: The Influence of Anisotropic Cues on Cell Behavior. *Front. Mater.* **2015**, *2*, 39. [[CrossRef](#)]
26. Curtis, R.; Ulrich, J.; Montaser, A.; Prausnitz, J.; Blanch, H. Protein-Protein Interactions in Concentrated Electrolyte Solutions: Hofmeister-Series Effects. *Biotechnol. Bioeng.* **2002**, *79*, 367–380. [[CrossRef](#)] [[PubMed](#)]
27. Rasidek, N.A.M.; Nordin, M.F.M.; Iwamoto, K.; Rahman, N.A.; Nagatsu, Y.; Tokuyama, H. Rheological Flow Models of Banana Peel Pectin Jellies as Affected by Sugar Concentration. *Int. J. Food Prop.* **2018**, *21*, 2087–2099. [[CrossRef](#)]
28. Kazemi, M.; Khodaiyan, F.; Hosseini, S.S. Utilization of Food Processing Wastes of Eggplant as a High Potential Pectin Source and Characterization of Extracted Pectin. *Food Chem.* **2019**, *294*, 339–346. [[CrossRef](#)] [[PubMed](#)]
29. Rwei, S.-P.; Chen, S.-W.; Mao, C.-F.; Fang, H.-W. Viscoelasticity and Wearability of Hyaluronate Solutions. *Biochem. Eng. J.* **2008**, *40*, 211–217. [[CrossRef](#)]
30. Kobayashi, T.; Nagai, T.; Suzuki, T.; Nosaka, Y.; Fujii, N. Restricted Permeation of Dextranulfates by Electrostatic Barrier of Negatively Charged Ultrafiltration Membranes: Salt Effect on the Permeation. *J. Memb. Sci.* **1994**, *86*, 47–56. [[CrossRef](#)]
31. Le, H.V.; Le Cerf, D. Colloidal Polyelectrolyte Complexes from Hyaluronic Acid: Preparation and Biomedical Applications. *Small* **2022**, *18*, 2204283. [[CrossRef](#)]
32. Wang, M.D.; Zhai, P.; Schreyer, D.J.; Zheng, R.S.; Sun, X.D.; Cui, F.Z.; Chen, X.B. Novel Crosslinked Alginate/Hyaluronic Acid Hydrogels for Nerve Tissue Engineering. *Front. Mater. Sci.* **2013**, *7*, 269–284. [[CrossRef](#)]
33. Bang, S.; Das, D.; Yu, J.; Noh, I. Evaluation of MC3T3 Cells Proliferation and Drug Release Study from Sodium Hyaluronate-1,4-Butanediol Diglycidyl Ether Patterned Gel. *Nanomaterials* **2017**, *7*, 328. [[CrossRef](#)] [[PubMed](#)]
34. Musilová, L.; Mráček, A.; Kašpárková, V.; Minařík, A.; Valente, A.J.M.; Azevedo, E.F.G.; Veríssimo, L.M.P.; Rodrigo, M.M.; Estesó, M.A.; Ribeiro, A.C.F. Effect of Hofmeister Ions on Transport Properties of Aqueous Solutions of Sodium Hyaluronate. *Int. J. Mol. Sci.* **2021**, *22*, 1932. [[CrossRef](#)] [[PubMed](#)]
35. Giubertoni, G.; Pérez de Alba Ortíz, A.; Bano, F.; Zhang, X.; Linhardt, R.J.; Green, D.E.; DeAngelis, P.L.; Koenderink, G.H.; Richter, R.P.; Ensing, B.; et al. Strong Reduction of the Chain Rigidity of Hyaluronan by Selective Binding of Ca²⁺ Ions. *Macromolecules* **2021**, *54*, 1137–1146. [[CrossRef](#)] [[PubMed](#)]
36. Havlíková, M.; Jugl, A.; Kadlec, M.; Smilek, J.; Chang, C.-H.; Pekař, M.; Mravec, F. Catanionic Vesicles and Their Complexes with Hyaluronan—A Way How to Tailor Physicochemical Properties via Ionic Strength. *J. Mol. Liq.* **2023**, *371*, 121089. [[CrossRef](#)]
37. Wójcik-Pastuszka, D.; Stawicka, K.; Dryś, A.; Musiał, W. Influence of HA on Release Process of Anionic and Cationic API Incorporated into Hydrophilic Gel. *Int. J. Mol. Sci.* **2023**, *24*, 5606. [[CrossRef](#)]
38. Bravo, B.; Correia, P.; Gonçalves Junior, J.E.; Sant’Anna, B.; Kerob, D. Benefits of Topical Hyaluronic Acid for Skin Quality and Signs of Skin Aging: From Literature Review to Clinical Evidence. *Dermatol. Ther.* **2022**, *35*, e15903. [[CrossRef](#)]

Disclaimer/Publisher’s Note: The statements, opinions and data contained in all publications are solely those of the individual author(s) and contributor(s) and not of MDPI and/or the editor(s). MDPI and/or the editor(s) disclaim responsibility for any injury to people or property resulting from any ideas, methods, instructions or products referred to in the content.